Noncoherent Physical-Layer Network Coding with FSK Modulation: Relay Receiver Design Issues

Matthew C. Valenti, *Senior Member, IEEE,* Don Torrieri, *Senior Member, IEEE,*
and Terry Ferrett, *Student Member, IEEE*

***Abstract*—A channel-coded physical-layer network coding strategy is refined for practical operation. The system uses frequency-shift keying (FSK) modulation and operates noncoherently, providing advantages over coherent operation: there are no requirements for perfect power control, phase synchronism, or estimates of carrier-phase offset. In contrast with *analog* network coding, which relays received analog signals plus noise, the system relays *digital* network codewords, obtained by digital demodulation and channel decoding at the relay. The emphasis of this paper is on the relay receiver formulation. Closed-form expressions are derived that provide bitwise log-likelihood ratios, which may be passed through a standard error-correction decoder. The role of fading-amplitude estimates is investigated, and an effective fading-amplitude estimator is developed. Simulation results are presented for a Rayleigh block-fading channel, and the influence of block length is explored. An example realization of the proposed system demonstrates a 32.4% throughput improvement compared to a similar system that performs network coding at the link layer. By properly selecting the rates of the channel codes, this benefit may be achieved without requiring an increase in transmit power.**

***Index Terms*—Network coding, two-way relay channel, frequency-shift keying, noncoherent reception, channel estimation.**

I. Introduction

In the two-way relay channel (TWRC), a pair of source *terminals* exchange information through an intermediate *relay* without a direct link between the sources [1]. The exchange can occur in two, three, or four orthogonal time slots, depending on how the information is encoded [2]. With a *traditional transmission scheduling scheme*, the exchange requires four slots. In each of the first two slots, one of the terminals transmits a packet to the relay, while in each of the last two slots, the relay transmits a packet to each of the terminals. By using *network coding* [3], the number of slots can be reduced. With *link-layer network coding* (LNC), the third and fourth slots are combined into one slot by having the relay add (modulo-2) the packets that it receives from the two terminals. During the third step, the relay sends the sum of the two packets, and each terminal is able to recover the information from the other terminal by subtracting (or adding, modulo-2) its own packet from the received signal. With *physical-layer network coding* (PNC), the first two slots are combined by having the two terminals transmit their packets at the same time [2]. The relay receives a combination of both modulated packets during the first slot, which it broadcasts (after appropriate processing) to the two terminals during the second slot. PNC-based strategies capable of supporting more than just two source terminals over the TWRC may be found in [4].

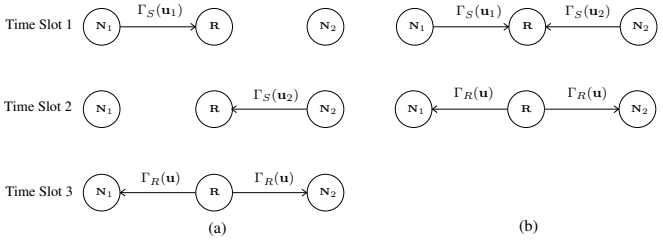

Fig. 1. (a) Link-layer network coding, and (b) Physical-layer network coding.

The transmission schedules for LNC and PNC are illustrated in Fig. 1. The source terminals $\mathcal{N}_1$ and $\mathcal{N}_2$ transmit messages $\mathbf{u}_1$ and $\mathbf{u}_2$, respectively, where each message is a packet containing many information bits. The messages are (channel) encoded and modulated by the function $\Gamma_S(\cdot)$. In the case of LNC, the two messages are sent in orthogonal time slots, while in the case of PNC, they are sent to the relay at the same time over a multiple-access channel (MAC). For both LNC and PNC, the relay broadcasts the encoded and modulated signal $\Gamma_R(\mathbf{u})$ in the final time slot, where $\mathbf{u}$ is the *network codeword* and $\Gamma_R(\cdot)$ is the function used by the relay to encode and modulate the network codeword. Using the received version of $\Gamma_R(\mathbf{u})$ and knowledge of its own message, each terminal is able to estimate the message sent by the other terminal.

There are several options for implementing PNC. The relay may simply amplify and forward the signal received from the end nodes, without performing demodulation and decoding. This PNC scheme is referred to as *analog network coding* (ANC) in [5] and *PNC over an infinite field* (PNCI) in [6]. Another option is for the relay to perform demodulation and decoding in an effort to estimate the network codeword, which is remodulated and broadcast to the terminals. This scheme is simply called PNC in [2] and *PNC over a finite field* (PNCF) in [6], but in this paper we refer to it as *digital network coding* (DNC) to distinguish it from ANC. Under

Paper approved by G. Bauch, the Editor for MIMO, Coding and Relaying of the IEEE Communications Society. Manuscript received January 12, 2011; revised March 25, 2011.

Portions of this paper were presented at the IEEE Military Communication Conference (MILCOM), San Jose, CA, Oct. 2010.

M. C. Valenti's contribution was sponsored by the National Science Foundation under Award No. CNS-0750821, and by the United States Army Research Laboratory under Contract W911NF-10-0109.

M. C. Valenti and T. Ferrett are with West Virginia University, Morgantown, WV (e-mail: {valenti, terry.ferrett}@ieee.org).

D. Torrieri is with the US Army Research Laboratory, Adelphi, MD (e-mail: dtorr@arl.army.mil).

Digital Object Identifier 10.1109/TCOMM.2011.063011.110030

Report Documentation Page

Form Approved
OMB No. 0704-0188

1. REPORT DATE	2. REPORT TYPE	3. DATES COVERED
MAR 2011		**00-00-2011 to 00-00-2011**

4. TITLE AND SUBTITLE	5a. CONTRACT NUMBER
Noncoherent Physical-Layer Network Coding with FSK Modulation:Relay Receiver Design Issues	5b. GRANT NUMBER
	5c. PROGRAM ELEMENT NUMBER
6. AUTHOR(S)	5d. PROJECT NUMBER
	5e. TASK NUMBER
	5f. WORK UNIT NUMBER
7. PERFORMING ORGANIZATION NAME(S) AND ADDRESS(ES) **US Army Research Laboratory,,Adelphi,,MD**	8. PERFORMING ORGANIZATION REPORT NUMBER
9. SPONSORING/MONITORING AGENCY NAME(S) AND ADDRESS(ES)	10. SPONSOR/MONITOR'S ACRONYM(S)
	11. SPONSOR/MONITOR'S REPORT NUMBER(S)

12. DISTRIBUTION/AVAILABILITY STATEMENT
Approved for public release; distribution unlimited

13. SUPPLEMENTARY NOTES
See also ADA610492,IEEE Transactions on Communications, 59(9), 2595-2604 (2011)

14. ABSTRACT

15. SUBJECT TERMS

16. SECURITY CLASSIFICATION OF:			17. LIMITATION OF ABSTRACT	18. NUMBER OF PAGES	19a. NAME OF RESPONSIBLE PERSON
a. REPORT **unclassified**	b. ABSTRACT **unclassified**	c. THIS PAGE **unclassified**	**Same as Report (SAR)**	**11**	

many channel conditions, DNC offers enhanced performance over ANC. This is because the decoding operation at the relay helps DNC to remove noise from the MAC phase, while the noise is amplified by the relay when ANC is used. However, ANC avoids the computational complexity of demodulation and decoding at the relay.

Symbol timing is a critical consideration in systems employing PNC. Synchronization of the clocks and packet transmissions at the two source nodes can be achieved by network timing updates. These updates are routine in networks with scheduling mechanisms, such as cellular networks. When the propagation times of the signals from the sources differ, the symbols arrive at the relay misaligned. The timing offset is $\tau = \Delta_d/c$, where c is the speed of light, and Δ_d is the difference in link distances from the sources to the relay. For insignificant delay, we need $\tau << T_s/2$, where T_s denotes the symbol period. This constraint limits the symbol rate. As an example, assume $\Delta_d = 300$ meters. Then, $T_s >> 2\ \mu s$ is required, and the symbol rate is limited to 250 kilosymbols/s. An alternative is to delay the transmission of the node closer to the relay by τ. However, this requires tracking the distances between the sources and the relay.

A common assumption made in the PNC literature is that the signals are coherently demodulated and that perfect channel-state information (CSI) is available at the receivers. For instance, decode-and-forward relaying has been considered for binary phase-shift keying [7] and minimum-shift keying [8] modulations, but in both cases the relay must perform coherent reception. An amplify-and-forward protocol is considered in [9], which allows the decision to be deferred by the relay to the end-node, though detection is still coherent. When two signals arrive concurrently at a common receiver, neither coherent detection nor the cophasing of the two signals (so that they arrive with a constant phase offset) is practical. The latter would require preambles that detract from the overall throughput, stable phases, and small frequency mismatches. To solve this problem, frequency-shift keying (FSK) was proposed for DNC systems in [10] and [11]. A key benefit of using FSK modulation is that it permits noncoherent reception, which eliminates the need for phase synchronization. An alternative to noncoherent FSK is to use differential modulation, which has been explored in [12].

In PNC systems, it is desirable to protect the data with a channel code. The combination of channel coding and physical-layer network coding is considered in [13] In [11], we investigate the use of a binary turbo code in a noncoherent DNC system. When using a binary turbo code in a DNC system, the relay demodulator must be able to produce bitwise log-likelihood ratios (LLRs) that are introduced to the input of the channel decoder.

Channel estimation is an important issue, especially when a channel code is used. A training-based channel estimation scheme for PNC at the relay assuming amplify-and-forward operation is considered in [14]. The relay estimates channel parameters from training symbols and adapts its broadcast power in order to maximize the signal-to-noise ratio at the end nodes. Estimation of both channel gains in the two-way relay channel at the end nodes, rather than the relay, is considered in [15]. Novel channel estimators are presented which provide better performance than common techniques such as least-square and linear-minimum-mean-squared error estimation. In [16], we propose a blind channel estimator for the relay of the noncoherent DNC system.

In this paper, we investigate receiver-design issues related to the use of noncoherent FSK in DNC systems. While noncoherent FSK has been previously proposed for DNC sytems in [10], we make the following specific contributions:

1) We provide *closed-form* expressions for the relay receiver decision rule with different types of CSI. This is in contrast with [10], which resorted to numerical methods to solve the decision rule (see the comment below equation (8) in [10]).
2) We consider the use of a turbo code for additional data protection. This requires that the relay receiver be formulated so that it produces bitwise LLRs, which may be passed through a standard turbo decoder.
3) We provide results for Rayleigh block-fading channels. The results in [10] were only for a phase-fading channel.
4) We propose a channel estimator that is capable of determining the fading amplitudes of the channels from the two terminals to the relay. The estimator does not require pilot symbols.

The remainder of this paper is organized as follows. Section II presents the system model used throughout the paper. Section III derives the relay receiver, while Section IV discusses channel-estimation issues. Section V provides simulation results, and Section VI concludes the paper.

II. System Model

The discrete-time system model shown in Fig. 2 gives an overview of the processing at all three nodes. Terminal $\mathcal{N}_i, i \in \{1,2\}$, generates a length-$K$ information sequence, $\mathbf{u}_i = [u_{i,1}, ..., u_{i,K}]$. The two terminals channel-encode and modulate their information sequences using the function $\Gamma_S(\cdot)$, which is common to both nodes. A rate-r_1 turbo code is used, and the resulting length $L_S = K/r_1$ turbo codeword generated by $\mathcal{N}_i$ is denoted by $\mathbf{b}_i = [b_{i,1}, ...b_{i,L_S}]$ (not shown in the diagram). The signal transmitted by node $\mathcal{N}_i$ during signaling interval $kT_s \le t \le (k+1)T_s$ is

$$s_i(t) = \sqrt{\frac{2\mathcal{E}_i}{T_s}} \cos\left[2\pi\left(f_{c_i} + \frac{b_{i,k}}{T_s}\right)(t - kT_s)\right] \quad (1)$$

where $\mathcal{E}_i$ is the transmit energy, f_{c_i} is the carrier frequency of node $\mathcal{N}_i$ (in practice, the carrier frequencies of the two nodes are not necessarily the same), and T_s is the symbol period. Note that (1) is continuous-phase frequency-shift keying (CPFSK) with a unity modulation index, which is orthogonal under noncoherent demodulation and has a continuous phase transition from one symbol to the next [17]. The orthogonally-modulated signal $s_i(t)$ may be represented in discrete time by the $2 \times L_S$ matrix $\mathbf{X}_i = [\mathbf{x}_{i,1}, ..., \mathbf{x}_{i,L_S}]$ with k^{th} column

$$\mathbf{x}_{i,k} = \begin{cases} [\ 1\ \ 0\ ]^T & \text{if } b_{i,k} = 0 \\ [\ 0\ \ 1\ ]^T & \text{if } b_{i,k} = 1. \end{cases} \quad (2)$$

For the DNC system, the signals are transmitted simultaneously by the two source nodes over a MAC channel. The relay receives the noisy electromagnetic sum of interfered and

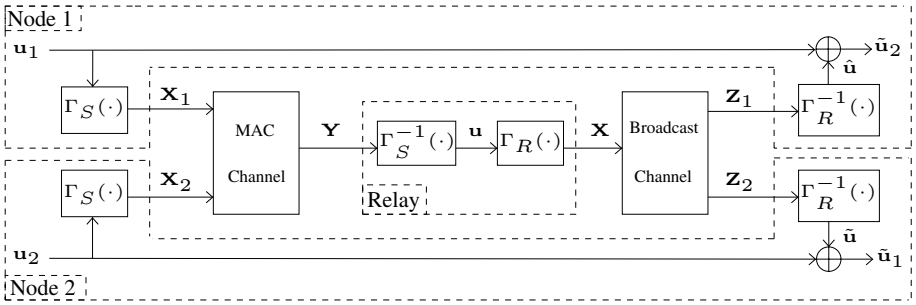

Fig. 2. Discrete-time system model.

faded signals, $\mathbf{Y}$, and applies the demodulation and channel-decoding function $\Gamma_S^{-1}(\cdot)$. The demodulation operation yields a soft estimate of the network-and-channel-coded message $\mathbf{b} = \mathbf{b}_1 \oplus \mathbf{b}_2$ (not shown), while the channel-decoding operation yields a hard-decision on the network-coded message $\mathbf{u} = \mathbf{u}_1 \oplus \mathbf{u}_2$. With the LNC system, the two sources transmit during orthogonal time slots. The received versions of $\mathbf{X}_1$ and $\mathbf{X}_2$ are demodulated independently to provide soft estimates of $\mathbf{b}_1$ and $\mathbf{b}_2$. These soft estimates are combined and turbo decoded to yield a hard estimate of $\mathbf{u}$. The key distinction between DNC and LNC is that with the DNC system, the estimate of $\mathbf{b}$ is obtained directly from $\mathbf{Y}$, while with LNC it is found by independently demodulating the two source signals and then combining them.

During the broadcast phase, the relay encodes and modulates $\mathbf{u}$ using the function $\Gamma_R(\cdot)$, which may be different than the function $\Gamma_S(\cdot)$ used by the sources. The channel code applied by the relay is a rate-r_2 turbo code, yielding a length $L_R = K/r_2$ turbo codeword. The code rates r_1 and r_2 used by the sources and relays, respectively, do not need to be the same. In the simulation results, we contemplate using a stronger code for the MAC phase than the broadcast phase, i.e. $r_1 < r_2$. The relay broadcasts its encoded and modulated signal, which may be represented in discrete-time by the $2 \times L_R$ matrix $\mathbf{X}$. The signal traverses two independent fading channels, and the end nodes receive independently faded versions of $\mathbf{X}$: $\mathbf{Z}_1$ at $\mathcal{N}_1$ and $\mathbf{Z}_2$ at $\mathcal{N}_2$. The end nodes demodulate and decode their received signals using the function $\Gamma_R^{-1}(\cdot)$, and form estimates of $\mathbf{u}$. Let $\hat{\mathbf{u}}$ denote the estimate at $\mathcal{N}_1$ and $\tilde{\mathbf{u}}$ denote the estimate at $\mathcal{N}_2$. Next, estimates of the transmitted information messages are formed, $\tilde{\mathbf{u}}_2 = \hat{\mathbf{u}} \oplus \mathbf{u}_1$ at $\mathcal{N}_1$ and $\tilde{\mathbf{u}}_1 = \tilde{\mathbf{u}} \oplus \mathbf{u}_2$ at $\mathcal{N}_2$. Since the links in the broadcast phase are conventional point-to-point links, specific details of the receiver formulation will not be presented here. A detailed exposition of receiver design for turbo-coded CPFSK systems in block fading channels can be found in [18].

All of the channels in the system are modeled as *block-fading* channels. A block is defined as a set of N symbols that all experience the same fading amplitude. The duration of each block corresponds roughly to the channel coherence time. Ideally both sources transmit with the same carrier frequency $f_{c_1} = f_{c_2}$. However, due to instabilities in each source node's oscillator and different Doppler shifts due to independent motion, it is not feasible to assume that these two frequencies are the same at the relay receiver. At best, the relay receiver could lock onto one of the two frequencies, in which case the received phase of the other signal would drift from one symbol to the next. To model this behavior, we let the phase shift within a block vary independently from symbol to symbol.

The signal matrix $\mathbf{X}_i$ transmitted by node $\mathcal{N}_i$ may be partitioned into $N_b = L_S/N$ blocks according to

$$\mathbf{X}_i \quad = \quad \left[\begin{array}{ccc} \mathbf{X}_i^{(1)} & \ldots & \mathbf{X}_i^{(N_b)} \end{array} \right] \tag{3}$$

where each block $\mathbf{X}_i^{(\ell)}, 1 \le \ell \le N_b$, is a $2 \times N$ matrix, and N_b is assumed to be an integer. The channel associated with block $\mathbf{X}_i^{(\ell)}$ is represented by the $N \times N$ diagonal matrix

$$\mathbf{H}_i^{(\ell)} \quad = \quad \alpha_i^{(\ell)} \times \text{diag}(\exp\{j\theta_{i,1}^{(\ell)}\}, \ \ldots, \exp\{j\theta_{i,N}^{(\ell)}\}) \tag{4}$$

where $\alpha_i^{(\ell)}$ is a real-valued fading amplitude and $\theta_{i,k}^{(\ell)}$ is the phase shift of the k^{th} symbol. The $\{\theta_{i,k}^{(\ell)}\}$ are independent and identically distributed over the interval $[0, 2\pi)$. The $\{\alpha_i^{(\ell)}\}$ are normalized so that $\mathcal{E}_i$ represents the average energy of terminal $\mathcal{N}_i$ received by the relay. The ℓ^{th} block at the sampled output of the relay receiver's matched-filters is then

$$\mathbf{Y}^{(\ell)} \quad = \quad \mathbf{X}_1^{(\ell)}\mathbf{H}_1^{(\ell)} + \mathbf{X}_2^{(\ell)}\mathbf{H}_2^{(\ell)} + \mathbf{N}^{(\ell)} \tag{5}$$

where $\mathbf{N}^{(\ell)}$ is a $2 \times N$ noise matrix whose elements are i.i.d. circularly-symmetric complex Gaussian random variables with zero mean and variance N_0.

III. Relay Receiver

At the relay, each block $\mathbf{Y}^{(\ell)}$ of the channel observation matrix $\mathbf{Y}$ is passed to a channel estimator, which computes estimates of the $\alpha_1^{(\ell)}$ and $\alpha_2^{(\ell)}$. A full description of the estimator is given in Section IV. The fading-amplitude estimates and channel observations are used to obtain soft estimates of the network-and-channel-coded sequence $\mathbf{b}$. The demodulator operates on a symbol-by-symbol basis, and therefore we may focus on a single signaling interval by dropping the dependence on the symbol interval k and the block index ℓ. Let b_1 and b_2 be the turbo-coded bits transmitted by terminals $\mathcal{N}_1$ and $\mathcal{N}_2$, and let $b = b_1 \oplus b_2$ be the corresponding network-coded bit. The relay demodulator computes the LLR

$$\Lambda(b) \quad = \quad \log \frac{P(b=1|\mathbf{y})}{P(b=0|\mathbf{y})} = \log \frac{P(b_1 \oplus b_2 = 1|\mathbf{y})}{P(b_1 \oplus b_2 = 0|\mathbf{y})} \tag{6}$$

where $\mathbf{y}$ is the corresponding column of $\mathbf{Y}$. The event $\{b_1 \oplus b_2 = 1\}$ is equivalent to the union of the events $\{b_1 = 0, b_2 = 1\}$ and $\{b_1 = 1, b_2 = 0\}$. Similarly, the event $\{b_1 \oplus b_2 = 0\}$

is equivalent to the union of the events $\{b_1 = 0, b_2 = 0\}$ and $\{b_1 = 1, b_2 = 1\}$. It follows that

$$\begin{aligned}\Lambda(b) &= \log \frac{P\left(\{b_1 = 0, b_2 = 1\} \cup \{b_1 = 1, b_2 = 0\}|\mathbf{y}\right)}{P\left(\{b_1 = 0, b_2 = 0\} \cup \{b_1 = 1, b_2 = 1\}|\mathbf{y}\right)} \\ &= \log \frac{P\left(\{b_1 = 0, b_2 = 1\}|\mathbf{y}\right) + P\left(\{b_1 = 1, b_2 = 0\}|\mathbf{y}\right)}{P\left(\{b_1 = 0, b_2 = 0\}|\mathbf{y}\right) + P\left(\{b_1 = 1, b_2 = 1\}|\mathbf{y}\right)}\end{aligned} \tag{7}$$

where the second line follows from the first because the events are mutually exclusive.

A. LNC Receiver

In the LNC system, the LLR's of b_1 and b_2 are first computed independently during the orthogonal time slots and are then combined according to the rules of LLR arithmetic. The LLR of the signal sent from node $\mathcal{N}_i$ to the relay is

$$\Lambda(b_i) \quad = \quad \log \frac{P(b_i = 1|\mathbf{y})}{P(b_i = 0|\mathbf{y})} \tag{8}$$

where $\mathbf{y}$ is the signal received during the time slot that node $\mathcal{N}_i$ transmits. When the fading amplitudes $\alpha_i, i = 1, 2$, are known, but the phases $\theta_i, i = 1, 2$, are not known, then (8) is found using [19]

$$\Lambda(b_i) \quad = \quad \log I_0\left(\frac{2\alpha_i|y_2|}{N_0}\right) - \log I_0\left(\frac{2\alpha_i|y_1|}{N_0}\right) \tag{9}$$

where $I_0(\cdot)$ is the zeroth-order Bessel function of the first kind and y_1 and y_2 are the components of $\mathbf{y}$. If the fading amplitudes are not known, but have Rayleigh distributions, then (8) is found using [19]

$$\Lambda(b_i) \quad = \quad \frac{\left(\mathcal{E}_i/N_0\right)^2}{1 + \mathcal{E}_i/N_0}\left\{|y_2|^2 - |y_1|^2\right\}. \tag{10}$$

Once the individual LLR's from each end node are found using (9) or (10), the LLR of the LNC system's network codeword can then be found from (7) and the independence of b_1 and b_2 when $\mathbf{y}$ is given:

$$\begin{aligned}\Lambda(b) &= \log \frac{e^{\Lambda(b_1)} + e^{\Lambda(b_2)}}{1 + e^{\Lambda(b_1)+\Lambda(b_2)}} \\ &= \max*\left[\Lambda(b_1), \Lambda(b_2)\right] - \max*\left[0, \Lambda(b_1) + \Lambda(b_2)\right]\end{aligned} \tag{11}$$

where $\max*[x, y] = \log(e^x + e^y)$.

B. PNC Receiver

In the PNC system, it is not sensible to compute $\Lambda(b_1)$ and $\Lambda(b_2)$ separately. Instead, use (7) and assume that the four events are equally likely along with Bayes' rule to obtain

$$\begin{aligned}\Lambda(b) = &\log\left[p\left(\mathbf{y}|\{b_1 = 0, b_2 = 1\}\right) + p\left(\mathbf{y}|\{b_1 = 1, b_2 = 0\}\right)\right] \\ &- \log\left[p\left(\mathbf{y}|\{b_1 = 0, b_2 = 0\}\right) + p\left(\mathbf{y}|\{b_1 = 1, b_2 = 1\}\right)\right].\end{aligned} \tag{12}$$

The computation of each $p\left(\mathbf{y}|\{b_1, b_2\}\right)$ by the PNC relay receiver given various levels of channel state information is the subject of the remainder of this section.

1) Coherent PNC Receiver: When the fading amplitudes and phases are known, $p\left(\mathbf{y}|\{b_1, b_2\}\right)$ is conditionally Gaussian. The mean is a two-dimensional complex vector whose value depends on the values of $\{b_1, b_2\}$ and the complex fading coefficients $\{h_1, h_2\}$, which are the corresponding entries of the $\mathbf{H}$ matrix. Let $\mathbf{m}[b_1, b_2]$ be the mean of $\mathbf{y}$ for the given values of b_1 and b_2. When $b_1 \neq b_2$, the two terminals transmit different frequencies and

$$\begin{aligned}\mathbf{m}[0, 1] &= \begin{bmatrix} h_1 & h_2 \end{bmatrix}^T \\ \mathbf{m}[1, 0] &= \begin{bmatrix} h_2 & h_1 \end{bmatrix}^T.\end{aligned} \tag{13}$$

When $b_1 = b_2$, the two terminals transmit the same frequency and

$$\begin{aligned}\mathbf{m}[0, 0] &= \begin{bmatrix} (h_1 + h_2) & 0 \end{bmatrix}^T \\ \mathbf{m}[1, 1] &= \begin{bmatrix} 0 & (h_1 + h_2) \end{bmatrix}^T.\end{aligned} \tag{14}$$

Since there is a one-to-one correspondence between the event $\{b_1, b_2\}$ and the mean vector $\mathbf{m}[b_1, b_2]$, it is equivalent to write $p\left(\mathbf{y}|\{b_1, b_2\}\right)$ as $p\left(\mathbf{y}|\mathbf{m}[b_1, b_2]\right)$, where

$$p\left(\mathbf{y}|\mathbf{m}[b_1, b_2]\right) = \left(\frac{1}{\pi N_0}\right)^2 \exp\left\{-\frac{1}{N_0}\left\|\mathbf{y} - \mathbf{m}[b_1, b_2]\right\|^2\right\}. \tag{15}$$

The coherent receiver computes each of the $p\left(\mathbf{y}|\{b_1, b_2\}\right)$ required by (12) by substituting the corresponding $\mathbf{m}[b_1, b_2]$ defined by (13) and (14) into (15).

2) Noncoherent PNC Receiver with CSI: Suppose that the receiver does not know the *phases* of the elements of the complex-valued $\mathbf{m}[b_1, b_2]$ vectors, but does know the *magnitudes* of the elements. The knowledge of the magnitudes constitutes a type of *channel-state information* (CSI). Define $\boldsymbol{\mu}[b_1, b_2]$ to be the two-dimensional real vector whose elements are the magnitudes of the elements of the complex vector $\mathbf{m}[b_1, b_2]$. When $b_1 \neq b_2$, both frequencies are used, and

$$\begin{aligned}\boldsymbol{\mu}[0, 1] &= \begin{bmatrix} |h_1| & |h_2| \end{bmatrix}^T = \begin{bmatrix} \alpha_1 & \alpha_2 \end{bmatrix}^T \\ \boldsymbol{\mu}[1, 0] &= \begin{bmatrix} |h_2| & |h_1| \end{bmatrix}^T = \begin{bmatrix} \alpha_2 & \alpha_1 \end{bmatrix}^T.\end{aligned} \tag{16}$$

When $b_1 = b_2$, only one frequency is used, and

$$\begin{aligned}\boldsymbol{\mu}[0, 0] &= \begin{bmatrix} |h_1 + h_2| & 0 \end{bmatrix}^T = \begin{bmatrix} \alpha & 0 \end{bmatrix}^T \\ \boldsymbol{\mu}[1, 1] &= \begin{bmatrix} 0 & |h_1 + h_2| \end{bmatrix}^T = \begin{bmatrix} 0 & \alpha \end{bmatrix}^T\end{aligned} \tag{17}$$

where $\alpha = |h_1 + h_2| = \sqrt{\alpha_1^2 + \alpha_2^2 + 2\alpha_1\alpha_2\cos(\theta_2 - \theta_1)}$.

The pdf of $\mathbf{y}$ conditioned on $\boldsymbol{\mu}[b_1, b_2]$ may be found by marginalizing over the unknown phases

$$p\left(\mathbf{y}|\boldsymbol{\mu}[b_1, b_2]\right) = \int_0^{2\pi}\int_0^{2\pi} p(\phi_1, \phi_2) p\left(\mathbf{y}|\mathbf{m}[b_1, b_2]\right) d\phi_1 d\phi_2. \tag{18}$$

where ϕ_1 and ϕ_2 are the phases of the first and second elements of $\mathbf{m}[b_1, b_2]$, respectively.

Assume that the α_i are Rayleigh distributed so that the h_i are circularly-symmetric zero-mean complex Gaussian*.

*The receiver derived in this subsection is valid even for non-Rayleigh fading, provided that the received phases over the two channels are independent and uniform over $(0, 2\pi)$.

When $b_1 \neq b_2$ each element of $\mathbf{m}[b_1, b_2]$ is a circularly-symmetric zero-mean complex Gaussian and therefore has uniform phase. On the other hand, when $b_1 = b_2$, one element is h_1+h_2, which is the sum of two circularly-symmetric zero-mean complex Gaussians, while the other element is zero. Since the sum of two circularly-symmetric complex Gaussians is also a circularly-symmetric complex Gaussian, it follows that $h_1 + h_2$ is a zero mean circularly-symmetric complex Gaussian and therefore its phase is uniform. Since the other element is zero, its phase is irrelevant and may be set to any arbitrary distribution, which is most conveniently chosen to be uniform. Thus, it follows that ϕ_1 and ϕ_2 are i.i.d. uniform. Therefore, the pdf conditioned on the magnitudes is

$$p\left(\mathbf{y}|\boldsymbol{\mu}[b_1,b_2]\right) = \frac{1}{\pi N_0}\int_0^{2\pi}\exp\left\{-\frac{|y_1-\mu_1[b_1,b_2]e^{j\phi_1}|^2}{N_0}\right\}d\phi_1 \times \frac{1}{\pi N_0}\int_0^{2\pi}\exp\left\{-\frac{|y_2-\mu_2[b_1,b_2]e^{j\phi_2}|^2}{N_0}\right\}d\phi_2 \quad (19)$$

where $\mu_k[b_1, b_2]$ is the k^{th} element of $\boldsymbol{\mu}[b_1, b_2]$ and

$$\frac{1}{2\pi}\int_0^{2\pi}\exp\left\{-\frac{|y_k-\mu_k[b_1,b_2]e^{j\phi_k}|^2}{N_0}\right\}d\phi_k = \exp\left\{-\frac{|y_k|^2+(\mu_k[b_1,b_2])^2}{N_0}\right\}I_0\left(\frac{2|y_k|\mu_k[b_1,b_2]}{N_0}\right). \quad (20)$$

Substituting (20) into (19),

$$p\left(\mathbf{y}|\boldsymbol{\mu}[b_1,b_2]\right) = \beta\prod_{k=1}^{2}\exp\left\{-\frac{(\mu_k[b_1,b_2])^2}{N_0}\right\} \times I_0\left(\frac{2|y_k|\mu_k[b_1,b_2]}{N_0}\right) \quad (21)$$

where

$$\beta = \left(\frac{2}{N_0}\right)^2\exp\left\{-\left(\frac{|y_1|^2+|y_2|^2}{N_0}\right)\right\} \quad (22)$$

which is common to all four $\{b_1, b_2\}$ and will therefore cancel in the LLR (12).

For each event $\{b_1, b_2\}$, substitute the $p\left(\mathbf{y}|\boldsymbol{\mu}[b_1, b_2]\right)$ given in (21) with the $\boldsymbol{\mu}[b_1, b_2]$ given by (16) and (17) as the corresponding $p\left(\mathbf{y}|\{b_1, b_2\}\right)$ in (12). This results in

$$\Lambda(b) = \log\left[e^{-\alpha_1^2/N_0}I_0\left(\frac{2\alpha_1|y_1|}{N_0}\right)e^{-\alpha_2^2/N_0}I_0\left(\frac{2\alpha_2|y_2|}{N_0}\right) + e^{-\alpha_2^2/N_0}I_0\left(\frac{2\alpha_2|y_1|}{N_0}\right)e^{-\alpha_1^2/N_0}I_0\left(\frac{2\alpha_1|y_2|}{N_0}\right)\right] - \log\left[e^{-\alpha^2/N_0}I_0\left(\frac{2\alpha|y_1|}{N_0}\right)+e^{-\alpha^2/N_0}I_0\left(\frac{2\alpha|y_2|}{N_0}\right)\right]. \quad (23)$$

As discussed in Section IV, it is possible to accurately estimate α_1 and α_2 in the considered block fading environment, provided the blocks are sufficiently long. However, it is not generally feasible to precisely estimate α because the phases θ_1 and θ_2 are varying on a symbol-by-symbol basis. Since $E[\cos(\theta_2 - \theta_1)] = 0$, a reasonable approximation when an estimate of α is not available is to use

$$\alpha \approx \sqrt{\alpha_1^2+\alpha_2^2}. \quad (24)$$

3) Noncoherent PNC Receiver without CSI: Suppose that besides not knowing the phases θ_1, θ_2, the relay receiver does not know the magnitude vector $\boldsymbol{\mu}[b_1, b_2]$. Then, the relay must operate without any channel state information except for the average energies $\mathcal{E}_1, \mathcal{E}_2$ and the noise variance N_0. When the magnitudes $\boldsymbol{\mu}[b_1, b_2]$ are not known, then the conditional pdf is found by marginalizing (21) over the unknown magnitudes

$$p\left(\mathbf{y}|\{b_1,b_2\}\right) = \int_0^\infty\int_0^\infty p(\mu_1,\mu_2)p\left(\mathbf{y}|\boldsymbol{\mu}[b_1,b_2]\right)d\mu_1 d\mu_2. \quad (25)$$

where μ_1 and μ_2 are the magnitudes of the first and second elements of $\boldsymbol{\mu}[b_1, b_2]$, respectively.

According to (16), when $b_1 \neq b_2$, one of the $\mu_k = \alpha_1$ while the other $\mu_k = \alpha_2$. Since α_1 and α_2 are independent and each α_i is Rayleigh with energy $\mathcal{E}_i$, it follows that the joint pdf of μ_1 and μ_2 when $(b_1, b_2) = (0, 1)$ is

$$p(\mu_1,\mu_2) = \left(\frac{2\mu_1}{\mathcal{E}_1}\exp\left\{-\frac{\mu_1}{\mathcal{E}_1}\right\}\right)\left(\frac{2\mu_2}{\mathcal{E}_2}\exp\left\{-\frac{\mu_2}{\mathcal{E}_2}\right\}\right) \quad (26)$$

for $\mu_1, \mu_2 \geq 0$, and when $(b_1, b_2) = (1, 0)$ it is

$$p(\mu_1,\mu_2) = \left(\frac{2\mu_1}{\mathcal{E}_2}\exp\left\{-\frac{\mu_1}{\mathcal{E}_2}\right\}\right)\left(\frac{2\mu_2}{\mathcal{E}_1}\exp\left\{-\frac{\mu_2}{\mathcal{E}_1}\right\}\right) \quad (27)$$

for $\mu_1, \mu_2 \geq 0$. Substituting (26) and (21) into (25) yields

$$p\left(\mathbf{y}|\{b_1=0,b_2=1\}\right) = \frac{|y_1|^2}{\frac{N_0^2}{\mathcal{E}_1}+N_0}+\frac{|y_2|^2}{\frac{N_0^2}{\mathcal{E}_2}+N_0} + \log\left[\left(\frac{1}{\mathcal{E}_1\mathcal{E}_2}\right)\left(\frac{1}{\mathcal{E}_1}+\frac{1}{N_0}\right)\left(\frac{1}{\mathcal{E}_2}+\frac{1}{N_0}\right)\right]^{-1}. \quad (28)$$

Similarly, substituting (27) and (21) into (25) yields

$$p\left(\mathbf{y}|\{b_1=1,b_2=0\}\right) = \frac{|y_1|^2}{\frac{N_0^2}{\mathcal{E}_2}+N_0}+\frac{|y_2|^2}{\frac{N_0^2}{\mathcal{E}_1}+N_0} + \log\left[\left(\frac{1}{\mathcal{E}_1\mathcal{E}_2}\right)\left(\frac{1}{\mathcal{E}_1}+\frac{1}{N_0}\right)\left(\frac{1}{\mathcal{E}_2}+\frac{1}{N_0}\right)\right]^{-1}. \quad (29)$$

As indicated by (17), when $b_1 = b_2$, one of the $\mu_k = \alpha$ while the other $\mu_k = 0$. As discussed below (18), in a Rayleigh-fading environment, h_1 and h_2 are independent, complex-valued, circularly-symmetric Gaussian variables, and therefore $h = h_1 + h_2$ is also a complex-valued, circularly-symmetric Gaussian variable. It follows that $\alpha = |h|$ is Rayleigh with energy $\mathcal{E}_1 + \mathcal{E}_2$, and the pdf of the nonzero μ_k is

$$p(\mu_k) = \frac{2\mu_k}{\mathcal{E}_1+\mathcal{E}_2}\exp\left\{-\frac{\mu_k}{\mathcal{E}_1+\mathcal{E}_2}\right\}, \quad \mu_k \geq 0. \quad (30)$$

For the $\mu_k = 0$, its pdf may be represented by an impulse at the origin, i.e. $p(\mu_k) = \delta(\mu_k)$. Substituting these pdfs with the appropriate $\boldsymbol{\mu}[b_1, b_2]$ into (25) yields

$$p\left(\mathbf{y}|\{b_1,b_2\}\right) = \log\left[\left(\frac{1}{\mathcal{E}_1+\mathcal{E}_2}\right)\left(\frac{1}{\mathcal{E}_1+\mathcal{E}_2}+\frac{1}{N_0}\right)\right]^{-1} + \frac{|y_i|^2}{\frac{N_0^2}{\mathcal{E}_1+\mathcal{E}_2}+N_0} \quad (31)$$

where $i = 1$ when $(b_1, b_2) = (0, 0)$ and $i = 2$ when $(b_1, b_2) = (1, 1)$.

Substituting (28) and (29) for the two $b_1 \neq b_2$ and (31) for the two $b_1 = b_2$ into (12) yields

$$\begin{aligned}\Lambda(b) &= \log\left[\frac{\xi_1\xi_2}{\xi N_0}\right] \\ &+ \log\left[\exp\left\{-\frac{|y_1|^2}{\xi} - \frac{|y_2|^2}{N_0}\right\} + \exp\left\{-\frac{|y_1|^2}{N_0} - \frac{|y_2|^2}{\xi}\right\}\right] \\ &- \log\left[\exp\left\{-\frac{|y_1|^2}{\xi_1} - \frac{|y_2|^2}{\xi_2}\right\} + \exp\left\{-\frac{|y_1|^2}{\xi_2} - \frac{|y_2|^2}{\xi_1}\right\}\right]\end{aligned} \tag{32}$$

where $\xi_1 = \mathcal{E}_1 + N_0$, $\xi_2 = \mathcal{E}_2 + N_0$, and $\xi = \mathcal{E}_1 + \mathcal{E}_2 + N_0$.

IV. Channel Estimator

The goal of the channel estimator is to estimate the values of the fading amplitudes α_1 and α_2 for a particular fading block. Let the fading amplitudes of a block be represented by the pair $\{A, B\}$, where $A \geq B$. Thus, $A = \max\{\alpha_1, \alpha_2\}$ and $B = \min\{\alpha_1, \alpha_2\}$. Note that in (23), exchanging α_1 and α_2 does not change the final expression. Therefore (23) is *commutative* in α_1 and α_2, and may be written as

$$\begin{aligned}\Lambda(b) = \max* &\left[F\left(\frac{2A|y_1|}{N_0}\right) + F\left(\frac{2B|y_2|}{N_0}\right),\right. \\ &\left. F\left(\frac{2B|y_1|}{N_0}\right) + F\left(\frac{2A|y_2|}{N_0}\right)\right] \\ - \max* &\left[F\left(\frac{2\sqrt{A^2+B^2}|y_1|}{N_0}\right), F\left(\frac{2\sqrt{A^2+B^2}|y_2|}{N_0}\right)\right]\end{aligned} \tag{33}$$

where the approximation $\alpha \approx \sqrt{\alpha_1^2 + \alpha_2^2}$ has been used and $F(x) = \log[I_0(x)]$, which may be efficiently and accurately computed through the following piecewise polynomial fit:

$$F(x) = \log[I_0(x)] \approx \begin{cases} 0.22594x^2 + 0.012495x - 0.0011272 & 0 < x \leq 1 \\ 0.12454x^2 + 0.21758x - 0.10782 & 1 < x \leq 2 \\ 0.028787x^2 + 0.63126x - 0.56413 & 2 < x \leq 5 \\ 0.003012x^2 + 0.88523x - 1.2115 & 5 < x \leq 15 \\ 0.00053203x^2 + 0.95304x - 1.6829 & 15 < x \leq 30 \\ 0.00013134x^2 + 0.97674x - 2.0388 & 30 < x \leq 60 \\ 0.9943x - 2.6446 & 60 < x \leq 120 \\ 0.99722x - 3.0039 & 120 < x \leq 500 \\ 0.99916x - 3.6114 & x > 500. \end{cases} \tag{34}$$

A. Fading Amplitude Estimator

To estimate A and B, first add the two elements of each $\mathbf{y}_i$ to obtain

$$r_i = y_{i,1} + y_{i,2} = h_{i,1} + h_{i,2} + \underbrace{n_{i,1} + n_{i,2}}_{\nu_i} \tag{35}$$

where ν_i is circularly-symmetric complex Gaussian noise with variance $2N_0$, and $h_{i,k}$ is the channel coefficient between terminal $\mathcal{N}_k, k = \{1, 2\}$, and the relay during the i^{th} signaling interval. The signal r_i is the noisy sum of two complex fading coefficients, and therefore the fading-amplitude estimation algorithm proposed by Hamkins in [20] may be used. To determine the values of A and B, a system of two equations with two unknowns is required. The first equation, found by taking the expected value of $|r_i|^2$ under the assumption that the fading amplitudes are fixed for the block in question, is

$$\begin{aligned}E\left[|r_i|^2\right] &= E\left[\alpha_1^2 + \alpha_2^2 + 2\alpha_1\alpha_2\cos(\theta_{i,2} - \theta_{i,1})\right] \\ &= E\left[\alpha_1^2 + \alpha_2^2\right] = \alpha_1^2 + \alpha_2^2 = A^2 + B^2.\end{aligned} \tag{36}$$

The second equation is found by conditioning on the event $\{|r|^2 > A^2 + B^2\}$, which is equivalent to $\{\cos(\theta_{i,2} - \theta_{i,1}) > 0\}$ and has expected value [20]

$$E\left[|r|^2 \middle| |r|^2 > A^2 + B^2\right] = A^2 + B^2 + \frac{4AB}{\pi}. \tag{37}$$

Solving (36) and (37) for A and B yields

$$\begin{aligned}A &= \frac{1}{2}\left(\sqrt{X + \frac{\pi}{2}(Y - X)} + \sqrt{X + \frac{\pi}{2}(X - Y)}\right) \\ B &= \frac{1}{2}\left(\sqrt{X + \frac{\pi}{2}(Y - X)} - \sqrt{X + \frac{\pi}{2}(X - Y)}\right)\end{aligned} \tag{38}$$

where $X = E\left[|r|^2\right]$ and $Y = E\left[|r|^2 \middle| |r|^2 > A^2 + B^2\right]$.

Since the expected values required for (38) are not known, they may be estimated by using the corresponding statistical averages,

$$\begin{aligned}\hat{X} &= \frac{1}{N}\sum_{i=1}^{N} |r_i|^2 \\ \hat{Y} &= \frac{2}{N}\sum_{i:|r_i|^2 > \hat{X}} |r_i|^2\end{aligned} \tag{39}$$

where N is the size of the fading block and the factor $2/N$ used to compute $\hat{Y}$ assumes that $|r_i|^2 > \hat{X}$ for approximately $N/2$ symbols. If this assumption is not true, then the multiplication by $2/N$ can be replaced with a division by the number of samples that satisfy $|r_i|^2 > \hat{X}$. As an alternative to summing over the $|r_i|^2 > \hat{X}$, Hamkins proposes summing over those $|r_i|^2$ greater than the median value of $\{|r_1|^2, ..., |r_N|^2\}$ [20].

The estimator works by computing estimates $\hat{X}$ and $\hat{Y}$ using (39) and the $\{r_1, ..., r_N\}$ for the block. These estimates are used in place of X and Y in (38), which yields estimates $\hat{A}$ and $\hat{B}$ of A and B. These estimates are then used in place of A and B in (33).

B. Transmission-Case Detection

According to (35), the two elements of $\mathbf{y}_i$ are always added together. When $b_1 = b_2$, only one tone is used, and the noise can be reduced if the receiver processes only the tone used and ignores the other tone. This requires that the receiver be able to detect whether the first tone, the second tone, or both tones were used, which may be implemented using a variation of the "no-CSI" receiver described in subsection III-B3. In [16], we contemplate an estimator that uses such a *transmission-case detector*. However, we found that the performances with and without the transmission-case detector were virtually identical and do not consider it further in this paper. At best, proper use of the transmission-case detector reduces the noise variance

from $2N_0$ to N_0 during the symbol intervals that both nodes transmit the same tone. As will be seen in the numerical results, the estimator is resilient enough against noise that this reduction in noise variance is not meaningful and does not justify the additional complexity.

C. Amplitude Estimation for Single-Transmitter Links

During the broadcast phase, there is only a single transmission, and the dual-amplitude estimator described in subsection IV-A is not necessary. Similarly, the estimator is not needed by the LNC system during the MAC phase since the two transmissions are over orthogonal channels. To estimate the fading amplitudes for the links involving only a single transmitter and receiver, the simple averaging technique given by (29) in [21] is used, which is described as follows. Consider the i^{th} signaling interval during the ℓ^{th} fading block. Given transmission of tone k, in the absence of noise, the k^{th} matched-filter output at the receiver is $y_{k,i} = \alpha e^{j\theta_i}$, and has magnitude $|y_{k,i}| = \alpha$. All other matched-filter outputs in the i^{th} signaling interval are 0. An estimate could be formed by taking the maximum $|y_{k,i}|$ over any column of $\mathbf{Y}_\ell$. In the presence of noise, an estimate of α can be formed by averaging across all columns of the fading block

$$\hat{\alpha} \quad = \quad \frac{1}{N}\sum_{i=1}^{N} \max_k |y_{k,i}|. \tag{40}$$

V. Simulation Study

This section presents simulated performance results for the relay receiver described in Section III. The simulated link model is as described in Section II, with specific simulation parameters given in the following subsections. The goal of the simulations is to compare the performance of comparable DNC and LNC systems and to assess the robustness of the channel estimator proposed in IV. Because the relay-broadcast phase of the DNC and LNC systems operate in exactly the same manner and have the same performance, we only focus on the performance of the MAC phase.

A. Uncoded Performance with Perfect Channel Estimates

We initially consider a system that does not use an outer error-correcting code, and thus $\mathbf{b}_i = \mathbf{u}_i, i = 1, 2$. We compare the performance of the LNC and DNC systems. With the LNC system, the two nodes transmit their messages in orthogonal time slots and the relay receiver first generates the individual LLR's during each time slot using either (9) or (10), and then the two LLR's are combined using (11). When there is no outer error-correcting code, performance using (9) is approximately the same as that using (10). A bit error is declared at the relay whenever a hard decision using (11) results in an erroneous decision on the corresponding bit of the network codeword $\mathbf{b}$. Such an error will usually occur if one of the two bits b_1, b_2 is received incorrectly, and therefore the error rate of the LNC system is approximately $P_b \approx 2p(1-p)$ where p is the bit error rate of noncoherent binary FSK modulation [17].

With the DNC system, the two nodes transmit simultaneously, and the relay receiver computes the LLR using (23) when the magnitudes $\boldsymbol{\mu}[b_1, b_2]$ are known or (32) when they are not. A hard decision is made on the LLR and a bit error is declared if the estimate of the corresponding network codeword bit b is incorrect. We assume that the channel estimates are perfect, and since there is no error-correction coding, the size of the fading block is irrelevant provided that the channel coherence time is not exceeded.

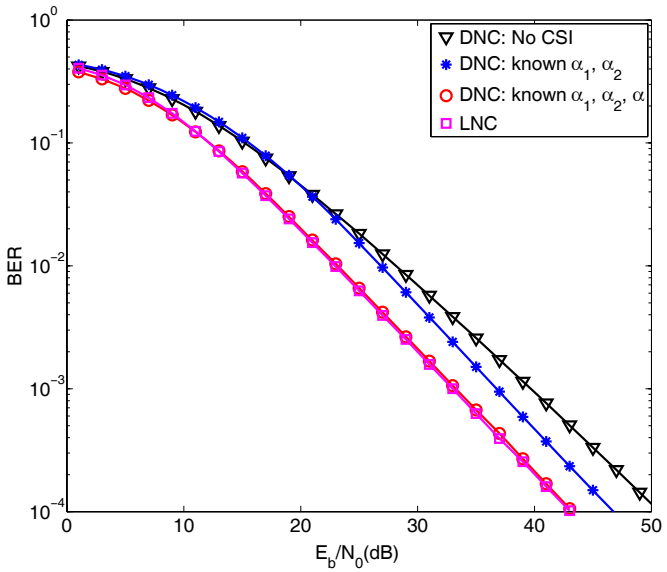

Fig. 3. Bit error rate at the relay in Rayleigh fading when DNC and LNC is used and $\mathcal{E}_2 = \mathcal{E}_1$. Depending on the amount of channel state information that is available, the PNC system will use one of three different relay receivers.

Initially, we set the average received energy to be the same over both channels, i.e. $\mathcal{E}_2 = \mathcal{E}_1 = \mathcal{E}_s = \mathcal{E}_b$. Fig. 3 shows the performance of the LNC and DNC systems in Rayleigh fading with equal energy signals. As anticipated, the LNC system offers the best performance, which is approximately 3 dB worse than a standard binary CPFSK system with noncoherent detection (the loss relative to conventional CPFSK is due to the fact that both bits must usually be received correctly). Three curves for the DNC system are shown in Fig. 3, corresponding to receivers that exploit different amounts of available channel state information. The best performance is achieved using a receiver implemented with (23), which requires knowledge of α_1, α_2, and α. The performance of the DNC system implemented with (23) is only about 0.25 dB worse than that of the LNC system. The worst performance is achieved using a receiver implemented using (32), which does not require knowledge of the fading amplitudes. The loss due to using (32) instead of (23) is about 10 dB, indicating that estimating the fading amplitudes at the relay is necessary.

While it may be feasible to estimate α_1 and α_2, estimating α may prove to be more difficult because it will depend on not only the individual fading amplitudes, but also on the phase difference between the two channels. Since the phase difference might change more quickly than the individual amplitudes, it might not be practical to estimate α. If that is the case, then the approximation given by (24) can be used in place of the actual value of α. The performance using this technique is also shown in Fig. 3 and shows a loss of about 3 dB with respect to the known-$\boldsymbol{\mu}[b_1, b_2]$ system, which requires knowledge of α.

The performance of DNC is sensitive to the balance of

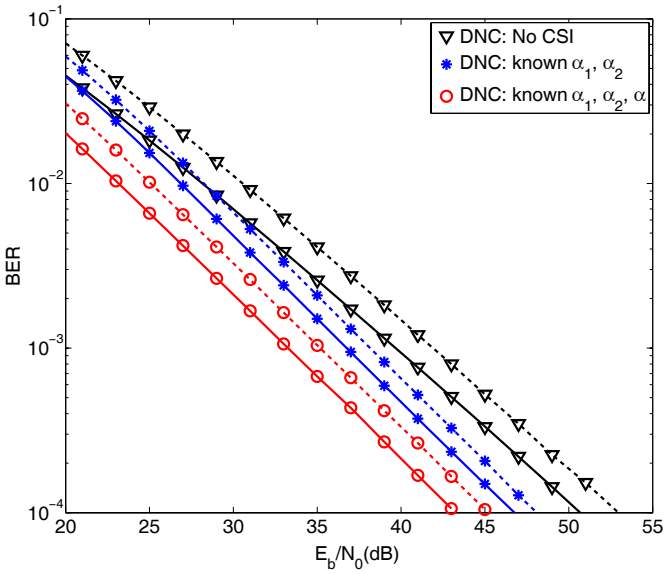

Fig. 4. Bit error rate at the relay in Rayleigh fading of DNC with three different receivers and either $\mathcal{E}_2 = \mathcal{E}_1$ (solid line) or $\mathcal{E}_2 = 4\mathcal{E}_1$ (dashed line).

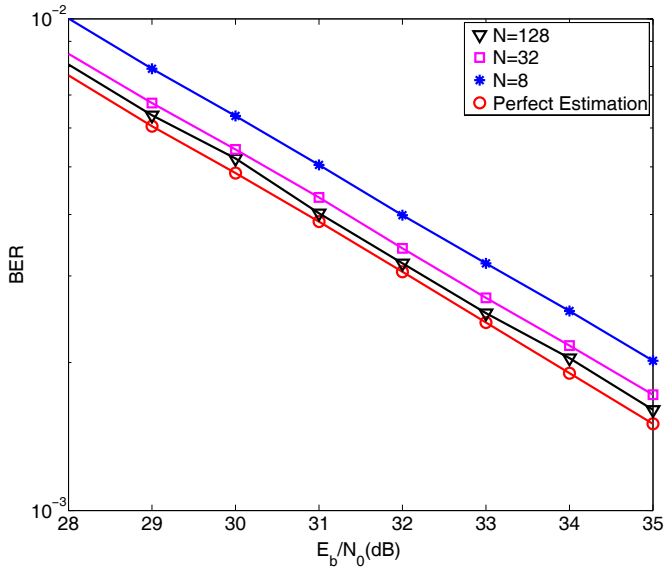

Fig. 5. Influence of fading-block length N on uncoded DNC error-rate performance at the relay. In addition to curves for three values of N, a curve is shown indicating the performance with perfect fading-amplitude knowledge.

power received over the two channels. Performance is best when $\mathcal{E}_1 = \mathcal{E}_2$. In order to evaluate how robust the DNC relay receivers are to an imbalance of power, the simulations were repeated with $\mathcal{E}_2 = 4\mathcal{E}_1$, while keeping $\mathcal{E}_b = \mathcal{E}_s = (\mathcal{E}_1+\mathcal{E}_2)/2$. These results are shown in Fig. 4 for the three receiver formulations that were considered in the previous figure. When the power is imbalanced in this way, there is a loss of about 2 dB. However, the loss is the same for all three receiver implementations, suggesting that they are robust to an imbalance of power.

B. Uncoded Performance with Channel Estimation

We now consider the influence of channel estimation, but still assume that the system does not use error-correction coding. In the simulations, the information frames generated at the end nodes contain $K = 2048$ bits per frame. The fading blocks are length $N = \{8, 32, 128\}$ symbols per block. The DNC relay implements (32) and then makes a hard decision on each information bit.

The bit error-rate performance of the uncoded system is shown in Fig. 5. The performance is shown with the estimator using the three block sizes $N = \{8, 32, 128\}$ as well as for the case of perfect estimates of α_1 and α_2. A narrow range of error rates is shown to better highlight the differences in performance. In general, smaller fading blocks lead to a less accurate estimation of the fading amplitudes, as the number of samples available for estimation decreases. Moving from block size $N = 128$ to 32 worsens performance by roughly 0.25 dB, and from $N = 32$ to 8 by 0.75 dB.

C. Performance with an Outer Turbo Code

Now consider a system that uses an outer turbo code. The terminals each encode length $K = 1229$ information sequences into length $L = 2048$ codewords, using a rate $r_1 \approx 0.6$ UMTS turbo code [22]. The relay performs turbo decoding using the codeword LLR's computed by (32). The

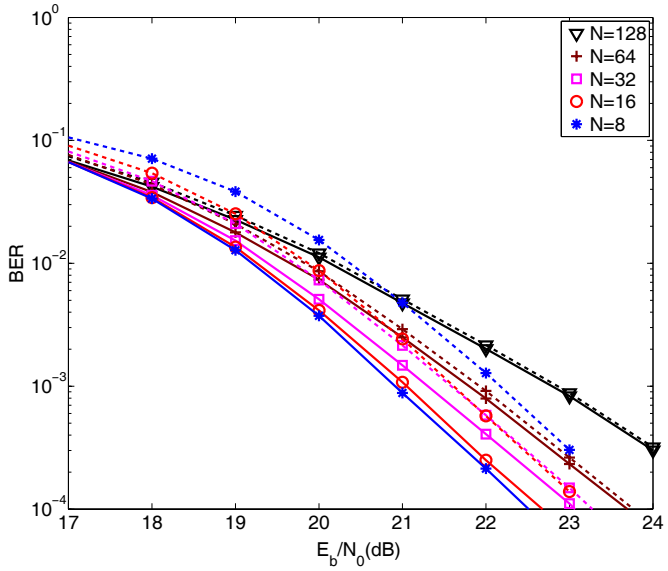

Fig. 6. Influence of fading-block length N on turbo-coded DNC error-rate performance at the relay. Two curves are shown for each value of $N = \{8,\ 16,\ 32,\ 64,\ 128\}$. Solid curves denote perfect fading-amplitude knowledge. Dashed curves denote estimated fading amplitudes.

fading-block lengths simulated are $N = \{8, 16, 32, 64, 128\}$ symbols per block.

The error performance of the coded system is shown in Fig. 6, both with perfect channel estimates and with estimated fading amplitudes. A good tradeoff between diversity and estimation accuracy is achieved for block sizes $N = 16$ and $N = 32$, which exhibit the best performance of all systems that must estimate the fading amplitudes. For $N < 16$ performance degrades due to the lack of enough observations per block for accurate channel estimates, while for $N > 32$ performance degrades due to the reduction in time diversity.

Fig. 7 shows the SNR required to reach an error rate of 10^{-4} at the relay as a function of the block length N. In each case, information is coded with the same $(2048, 1229)$ turbo code used for Fig. 6. Curves for three systems are shown: The noncoherent receiver with known $\{\alpha_1, \alpha_2\}$, the noncoherent

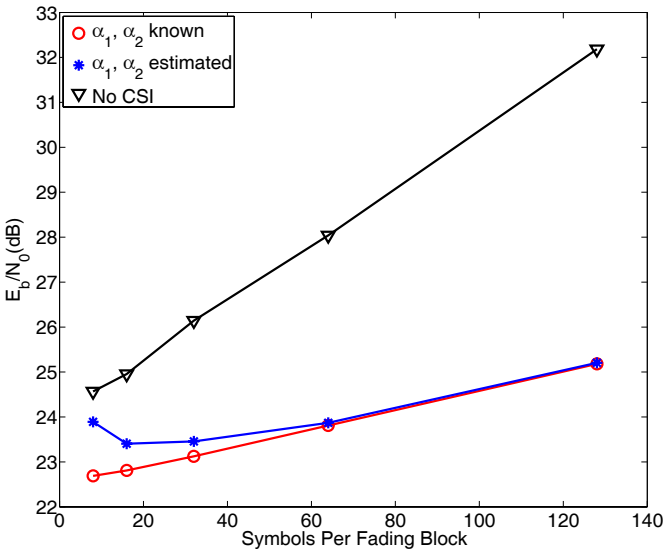

Fig. 7. Signal-to-noise ratio required to reach a bit error rate of 10^{-4} at the relay as a function of fading-block length. The performance of three systems is shown: The noncoherent receiver with known $\{\alpha_1, \alpha_2\}$, the noncoherent receiver with estimated $\{\alpha_1, \alpha_2\}$, and the noncoherent receiver that does not use CSI. All systems use a Turbo code with rate $1229/2048$.

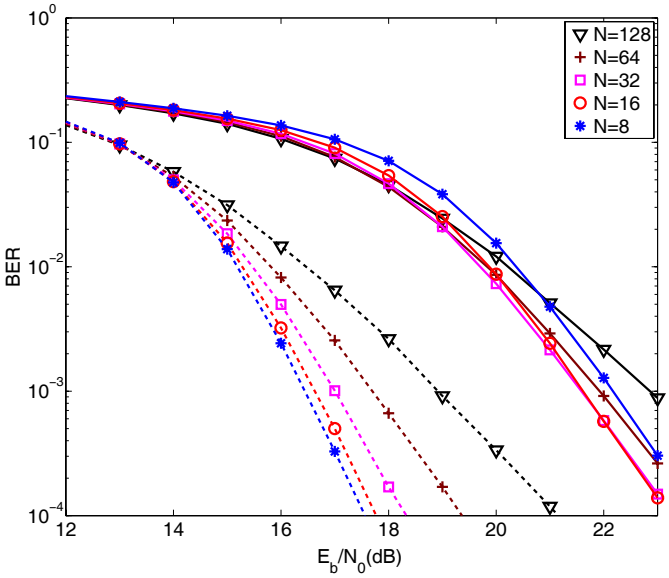

Fig. 8. Comparison of error-rate performance between the turbo-coded DNC and LNC systems at the relay. The solid lines denote DNC, while the dashed lines denote LNC.

receiver with estimated $\{\alpha_1, \alpha_2\}$, and the noncoherent receiver that does not use CSI. When $\{\alpha_1, \alpha_2\}$ are not estimated, performance improves with decreasing N because of the increased number of blocks per codeword, which increases the time diversity. However, when $\{\alpha_1, \alpha_2\}$ are estimated, the performance gets worse when the block size is smaller than $N = 16$. The loss of time diversity as the block size increases is a common problem for any system operating over a slow-fading channel, and the system proposed in this paper is no exception. The performance gap between the known-CSI and no-CSI receiver formulations widens with increasing block length.

An error-rate performance comparison between DNC and LNC is shown in Fig. 8. Both systems use the same $(2048, 1229)$ turbo code. The LNC system outperforms the

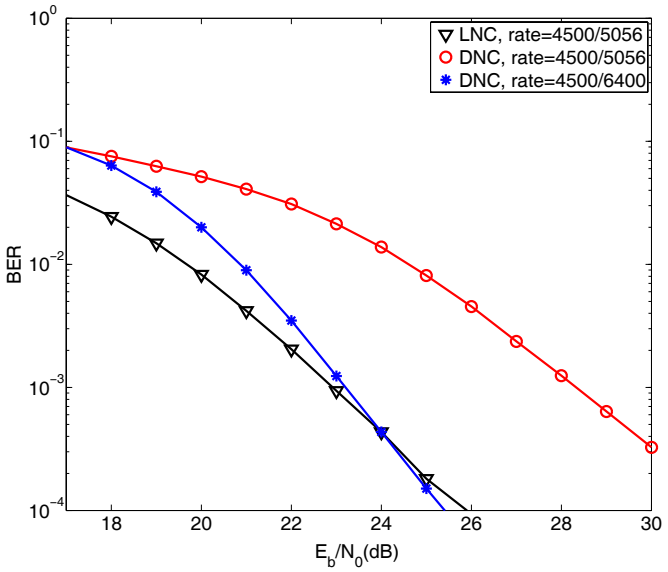

Fig. 9. Comparison of the performance of turbo-coded DNC and LNC at the relay with block size $N = 32$. For the DNC system, two code rates are shown, with the lower rate code offering comparable performance to the LNC system.

DNC system by margins ranging between 4 and 6 dB.

While the LNC system is more energy efficient than the DNC system when the same-rate turbo code is used, the throughput of the LNC system is worse than that of the DNC system because the two terminals must transmit in orthogonal time slots. The loss in energy efficiency from using DNC versus LNC can be recovered by having the source terminals use a lower-rate turbo code. Consider the performance comparison shown in Fig. 9 for block size $N = 32$. At $E_b/N_0 \approx 24$ dB, DNC using a rate $r_1 = 4500/6400$ code matches the error-rate performance of LNC using a rate $r_1 = 4500/5056$ code. Because the two terminals transmit at the same time, the end-to-end throughput of DNC is higher than that of LNC, even though the DNC terminals transmit to the relay with a lower-rate channel code.

To illustrate the throughput improvement of DNC over LNC, consider the following transmission schedule for the two systems. Assume the source terminals use rate $r_1 = 4500/6400$ in DNC, and $r_1 = 4500/5056$ in LNC. Assume operation at $E_b/N_0 = 24$ dB, yielding approximately equal relay error-rate performance. Further, assume that both systems use code rate $r_2 = 4500/5056$ for relay broadcast, yielding approximately equal end-to-end performance. DNC requires 6400 channel uses for transmission to the relay versus $2 \times 5056 = 10112$ for LNC. Both systems require 5056 channel uses for relay broadcast. The throughput for DNC is thus $T^{(DNC)} = 9000/(6400 + 5056) = 9000/11,456$ bits per channel use, and for LNC $T^{(LNC)} = 9000/(3 \times 5056) = 9000/15,168$ bits per channel use. The percentage throughput increase of DNC over LNC is thus $(T^{(DNC)}/T^{(LNC)} - 1) \times 100 \approx 32.4\%$.

VI. Conclusion

A throughput-improving technique for relaying in the two-way relay network, *digital network coding*, is refined for practical operation. The system operates noncoherently, providing advantages over coherent operation: there are no requirements

for perfect power control, phase synchronism, or estimates of carrier-phase offset.

A computationally simple technique for estimating fading amplitudes at the relay is implemented. Error-rate performance in the noncoherent Rayleigh block-fading channel at several block sizes is presented. The system is simulated with and without an outer error-correcting code. The coded error-rate performance of the system using estimation differs from that with ideal estimates by margins between $0.7 - 1.5$ dB.

When the same-rate turbo code is used, digital network coding has a higher throughput but lower energy-efficiency than link-layer network coding . The energy loss of DNC can be recovered by using a lower-rate turbo code during the MAC phase. Even when the loss of spectral efficiency due to the lower-rate turbo code is taken into account, the DNC system is able to achieve a higher throughput than LNC at the same energy-efficiency. In the particular example presented in this paper, the DNC system is capable of achieving throughputs that are 32.4% larger than that of the equivalent LNC system, while operating at the same energy efficiency.

REFERENCES

[1] B. Rankov and A. Wittneben, "Achievable rate regions for the two-way relay channel," in *Proc. Int. Symp. Inf. Theory*, pp. 1668-1672, July 2006.

[2] S. Zhang, S. C. Liew, and P. P. Lam, "Hot topic: physical-layer network coding," in *Proc. ACM Annual Int. Conf. Mobile Comput. Netw.*, pp. 358-365, Sep. 2006.

[3] R. Ahlswede, N. Cai, S. Li, and R. Yeung, "Network information flow," *IEEE Trans. Inf. Theory*, vol. 46, pp. 1204-1216, July 2000.

[4] M. Chen and A. Yener, "Multiuser two-way relaying: detection and interference management strategies," *IEEE Trans. Wireless Commun.*, vol. 8, no. 8, pp. 4296-4305, Aug. 2009.

[5] S. Katti, S. Gollakota, and D. Katabi, "Embracing wireless interference: analog network coding," in *Proc. ACM SIGCOMM*, pp. 397-408, Aug. 2007.

[6] S. Zhang, S. C. Liew, and L. Lu, "Physical layer network coding schemes over finite and infinite fields," in *Proc. IEEE Global Telecommun. Conf.*, pp. 1-6, Dec. 2008.

[7] E. Peh, Y. Liang, and Y. L. Guan, "Power control for physical-layer network coding in fading environments," in *Proc. IEEE Personal Indoor Mobile Radio Commun. Conf.*, pp. 1-5, 2008.

[8] S. Katti, H. Rahul, W. Hu, D. Katabi, M. Medard, and J. Crowcroft, "XORs in the air: practical wireless network coding," *IEEE/ACM Trans. Netw.*, pp. 497-510, June 2008.

[9] P. Popovski and H. Yomo, "Wireless network coding by amplify-and-forward for bi-directional traffic flows," *IEEE Commun. Lett.*, vol. 11, pp. 16-18, Jan. 2007.

[10] J. Sørensen, R. Krigslund, P. Popovski, T. Akino, and T. Larsen, "Physical layer network coding for FSK systems," *IEEE Commun. Lett.*, vol. 13, no. 8, pp. 597-599, Aug. 2009.

[11] M. C. Valenti, D. Torrieri, and T. Ferrett, "Noncoherent physical-layer network coding using binary CPFSK modulation," in *Proc. IEEE Military Commun. Conf.*, pp. 1-7, Oct. 2009.

[12] T. Cui, F. Gao, and C. Tellambura, "Physical layer differential network coding for two-way relay channels," in *Proc. IEEE Global Telecommun. Conf.*, Dec. 2008.

[13] S. Zhang and S. C. Liew, "Channel coding and decoding in a relay system operated with physical-layer network coding," *IEEE J. Sel. Areas Commun.*, vol. 27, pp. 788-789, June 2009.

[14] B. Jiang, F. Gao, X. Gao, and A. Nallanathan, "Channel estimation and training design for two-way relay networks with power allocation," *IEEE Trans. Wireless Commun.*, vol. 9, no. 6, pp. 2022-2032, June 2010.

[15] F. Gao, R. Zhang, and Y. C. Liang, "On channel estimation for amplify-and-forward two-way relay networks," in *Proc. IEEE Global Telecommun. Conf.*, Dec. 2008.

[16] T. Ferrett, M. C. Valenti, and D. Torrieri, "Receiver design for noncoherent digital network coding," in *Proc. IEEE Military Commun. Conf.*, Nov. 2010.

[17] J. G. Proakis and M. Salehi, *Digital Communications*, 5th edition. McGraw-Hill, Inc., 2008.

[18] S. Cheng, M. C. Valenti, and D. Torrieri, "Robust iterative noncoherent reception of coded FSK over block fading channels," *IEEE Trans. Wireless Commun.*, vol. 6, pp. 3142-3147, Sep. 2007.

[19] M. C. Valenti and S. Cheng, "Iterative demodulation and decoding of turbo coded M-ary noncoherent orthogonal modulation," *IEEE J. Sel. Areas Commun.*, vol. 23, pp. 1738-1747, Sep. 2005.

[20] J. Hamkins, "An analytic technique to separate cochannel FM signals," *IEEE Trans. Commun.*, vol. 48, pp. 543-546, Apr. 2000.

[21] D. Torrieri, S. Cheng, and M. C. Valenti, "Robust frequency hopping for interference and fading channels," *IEEE Trans. Wireless Commun.*, vol. 56, pp. 1343-1351, Aug. 2008.

[22] European Telecommunications Standards Institute, "Universal mobile telecommunications system (UMTS): multiplexing and channel coding (FDD)," 3GPP TS 25.212 version 7.4.0, June 2006.

Matthew C. Valenti is a Professor in Lane Department of Computer Science and Electrical Engineering at West Virginia University. He holds B.S. and Ph.D. degrees in Electrical Engineering from Virginia Tech and a M.S. in Electrical Engineering from the Johns Hopkins University. From 1992 to 1995 he was an electronics engineer at the U.S. Naval Research Laboratory. He serves as an associate editor for IEEE TRANSACTIONS ON WIRELESS COMMUNICATIONS and as co-chair of the Technical Program Committee for Globecom-2013, and has served as an editor for IEEE TRANSACTIONS ON VEHICULAR TECHNOLOGY and as track or symposium co-chair for the Fall 2007 VTC, ICC-2009, Milcom-2010, and ICC-2011. His research interests are in the areas of communication theory, error correction coding, applied information theory, wireless networks, simulation, and grid computing. His research is funded by the NSF and DoD.

Don Torrieri is a research engineer and Fellow of the US Army Research Laboratory. His primary research interests are communication systems, adaptive arrays, and signal processing. He received the Ph.D. degree from the University of Maryland. He is the author of many articles and several books including *Principles of Spread-Spectrum Communication Systems, 2nd ed.* (Springer, 2011). He teaches graduate courses at Johns Hopkins University and has taught many short courses. In 2004, he received the Military Communications Conference achievement award for sustained contributions to the field.

Terry Ferrett is a research assistant at West Virginia University, Morgantown, WV completing his Ph.D. degree in electrical engineering. He received the B.S. degrees in electrical engineering and computer engineering in 2005 and the M.S. degree in electrical engineering in 2008 from West Virginia University. He is the architect of a cluster computing resource utilized by electrical engineering students at West Virginia University to conduct communication theory research. His research interests are network coding, digital receiver design, the information theory of relay channels, cluster and grid computing, and software project management.